PdIn-Based Pseudo-Binary Alloy as a Catalyst for NO_x Removal Under Lean Conditions

Jaewan Jeon,† Hyungwon Ham,† Feilong Xing,† Yuki Nakaya,†Ken-ichi Shimizu,†,‡ Shinya Furukawa*,†,‡,§

† Institute for Catalysis, Hokkaido University, N21, W10, Sapporo 001-0021, Japan

‡ Elements Strategy Initiative for Catalysts and Batteries, Kyoto University, Katsura, Kyoto 615-8520, Japan

§ Japan Science and Technology Agency, PRESTO, Chiyodaku, Tokyo 102-0076, Japan

KEYWORDS: NO_x removal; lean condition; pseudo-binary alloy; intermetallic compound; PdIn

ABSTRACT: Developing a noble metal-based catalyst that works effectively for NO_x removal in the presence of excess O_2 is still a big challenge in catalytic chemistry for exhaust gas purification. To overcome this challenge, in this study, we designed and prepared a nanoparticulate $(Pd_{1-x}Pt_x)In$ pseudo-binary alloy using Al_2O_3 and CeO_2 supports, in which a part of Pd was replaced with Pt to improve the oxidation tolerance of In during NO_x reduction under lean conditions. Multiple characterization techniques were used to confirm the formation of the desired pseudo-binary alloy phase. The prepared Pd–Pt–In/CeO_2 catalyst exhibited high NO conversion to N_2 in NO–CO–O_2 reaction with a wide range of oxygen concentration including lean conditions (80%–100%, $0.75 \le \lambda \le 1.5$, 350 °C) and retained its catalytic performance during rich–lean cycles.

Nitrogen oxides (NO_x) generated as exhaust gas from internal combustion engines are known to cause air pollution (NO and NO_2)[1] and global warming (N_2O);[2] therefore, their emissions have been strictly restricted worldwide.[3] Three-way catalytic (TWC) systems using noble metals (Rh, Pd, and Pt) have been extensively used for the simultaneous conversion of NO_x, CO, and hydrocarbons, which are generated from gasoline engines, into N_2, CO_2, and H_2O.[4] Oxygen (air) concentration is the key factor for the simultaneous purification of these harmful gases because air-fuel equivalence ratios (λ) that are not stoichiometric lower purification efficiency.[5] Specifically, NO_x conversion considerably decreases when λ is higher than 1.01 (lean conditions).[5] This occurs because O_2[6] is more easily dissociated by noble metals than NO[7] to form O and oxidize reductants (CO or hydrocarbons), in which surplus NO_x remains. However, lean conditions are of significant benefit for fuel economy;[5] hence, developing a highly efficient catalytic system for NO_x removal that works even under lean conditions is important.[8] To overcome this challenge, the noble metal catalyst should be modified to suppress O_2 activation while maintaining the NO dissociation performance.

A possible candidate material to solve this issue is intermetallic PdIn with a CsCl-type structure (Figure 1). Recently, we have reported that intermetallic PdIn showed high catalytic performance for NO_x removal (both NO and N_2O).[9] Our kinetic and theoretical studies revealed that Pd and In catalyzed NO reduction to N_2 and N_2O, and the subsequent N_2O decomposition to N_2, respectively (Figure 1c), which allowed highly selective NO reduction to N_2 at various temperature regions.[9]

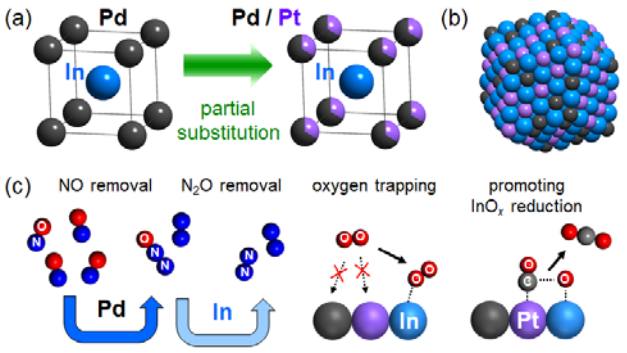

Figure 1. (a) Catalyst design based on intermetallic PdIn with Pd–Pt substitution for efficient NO_x removal under lean conditions. (b) Rhombohedral model nanoparticle of $(Pd_{1-x}Pt_x)In$ with {110} terminations. (c) Role of each metal in the catalysis.

In this study, oxophilic In is also expected to work as an oxygen trapping site to inhibit O_2 activation on noble metal sites (Figure 1c), which makes it a potential material for NO_x removal under lean conditions. However, metallic In on the surface is easily oxidized to InO_x species in the presence of oxidants,[9] which no longer retain the oxophilic character essential for the desired catalysis. Under stoichiometric or rich conditions, Pd can catalyze the reduction of InO_x by CO[9] or hydrocarbons,[10] which mostly retains the metallic state of In at the steady-state of continuous In–InO_x redox cycles.[9] However, for lean conditions, In cannot maintain its metallic state because of excess oxygen.[9-10] Therefore, the catalyst should have a much greater ability to reduce InO_x so that the higher oxidation tolerance of In is obtained. In this study, we focused on the use of Pt, which is known to promote the

reduction of metal oxides by CO (Figure 1c) or hydrogen more strongly than Pd.[11] Pt can be introduced to the PdIn system by applying the pseudo-binary alloy structure,[9, 12] where part of Pd is substituted by Pt without changing the parent CsCl-type structure (Figures 1a and 1b). This catalyst design allows the adjacency of Pd, Pt, and In on an atomic level, which would provide multifunctional active sites that are effective for NO_x removal under lean conditions. Herein, we report a novel catalytic system using a $(Pd_{1-x}Pt_x)In$ pseudo-binary alloy that works even under severe lean conditions of $\lambda = 1.5$.

The catalysts were prepared by the conventional co-impregnation method using γ-Al_2O_3 as a support (see Supplementary Information and Table S1 for the preparation method and detailed information on the catalysts, respectively). X-ray diffraction analysis for Pd–In/Al_2O_3 (Pd:In = 1:1) confirmed that the intermetallic PdIn phase was formed on Al_2O_3. However, for Pd–Pt–In/Al_2O_3 (Pd:Pt:In =0.5:0.5:1), the corresponding diffraction peak seemed to overlap with that of the support, which hampered phase assignment. Therefore, we conducted high-angle annular dark field scanning transmission electron microscopy (HAADF–STEM) and energy-dispersive X-ray (EDX) analyses of the Pd–Pt–In/Al_2O_3 catalyst (Figure 2).

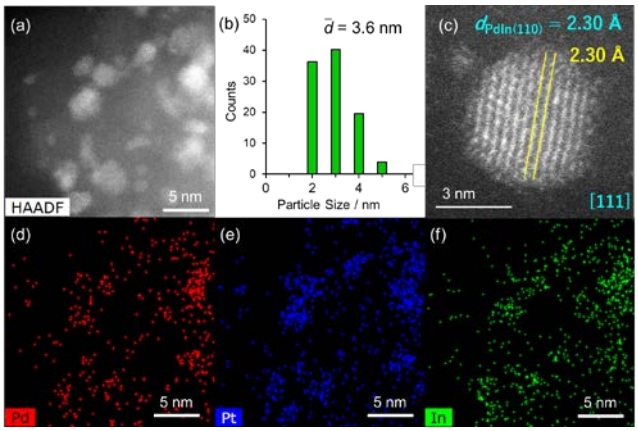

Figure 2. (a) HAADF–STEM image of Pd–Pt–In/Al_2O_3 and (b) the size distribution of nanoparticles. (c) Magnification of a single nanoparticle. Elemental maps of (d) Pd, (e) Pt, and (f) In acquired using EDX for the region designated in (a).

The particle sizes were in the range of 2–5 nm with a mean diameter of 3.6 nm. The high-resolution image of a single nanoparticle showed lattice fringes with a 2.30 Å spacing, which was consistent with the interplanar distance of the PdIn(110) plane (2.30 Å). The elemental maps of Pd, Pt, and In confirmed that these three elements comprising the nanoparticles were homogeneously dispersed. These results strongly indicate the formation of Pd–Pt–In trimetallic alloy nanoparticles with a PdIn-like structure. Considering that the atomic radii of Pd and Pt are similar (Pd: 1.373 Å, Pt 1.385 Å, and In: 1.660 Å), the lattice constant of PdIn and the resulting interplanar distance are unlikely to change even upon the Pd–Pt substitution. We also performed a Fourier-transform infrared (FT-IR) study with CO adsorption to investigate the surface structure.

FT-IR spectra of CO adsorbed on Pd- and Pt-based catalysts are shown in Figure 3. For monometallic Pd, adsorption bands,

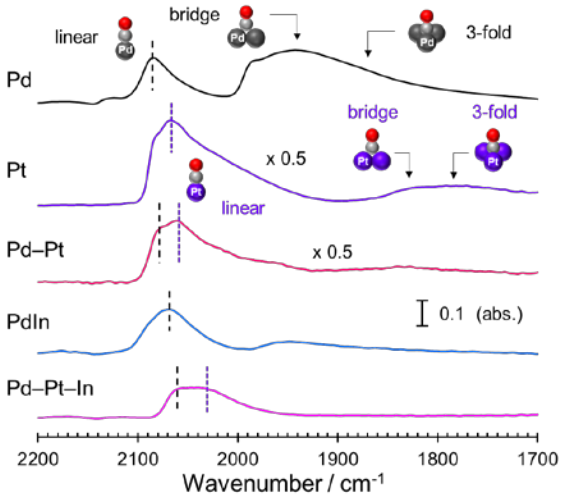

Figure 3. FT-IR spectra of CO adsorbed on various Al_2O_3-supported catalysts.

which are assignable to the stretching vibration of CO adsorbed with linear, bridge, and threefold modes, appeared at 2085, 1940, and 1870 cm^{-1}, respectively.[13] Similar adsorption bands were also observed for monometallic Pt (2067, 1820, and 1770 cm^{-1});[14] however, each peak position was lower than that of Pd. Pd–Pt alloy ($Pd_{0.5}Pt_{0.5}$) showed both features of Pd and Pt in the region of linear CO. Intermetallic PdIn produced a single peak of linear CO, whereas the intensities of multi-fold CO considerably decreased, which indicated that Pd–Pd ensembles were diluted upon the formation of the intermetallic phase. For Pd–Pt–In, two linear CO assignable to those on Pd and Pt appeared at lower wavenumbers than those for Pd–Pt alloy. This result indicates that both Pd and Pt are present at the surface and become electron-rich because of the ligand effect by In, as has been reported for PdIn.[9] Additionally, multi-fold CO species were not observed likely because of the formation of the PdIn-like intermetallic phase. Therefore, the FT-IR results suggest the adjacency of Pd, Pt, and In on an atomic level and their even distribution.

Next, X-ray adsorption fine structure (XAFS) analysis was conducted to further characterize the Pd–Pt–In catalyst. The Pd K-, Pt L_{III}-, and In K-edge X-ray adsorption near edge structure (XANES) spectra of Pd–Pt–In/Al_2O_3 showed similar features (adsorption edge and white line intensity) to those of reference foils (Figure S2), which confirmed that these metals were in the metallic state. The results of curve fitting for extended XAFS (EXAFS) oscillations for Pd–Pt–In/Al_2O_3 are summarized in Table 1 (see Figure S3 and Table S2 for the law EXAFS oscillation and fits, and the details of curve-fitting, respectively). For Pd K- and Pt L_{III}-edges, Pd–In and Pt–In scattering was observed with similar coordination numbers (*CN*s) and interatomic distances. The corresponding In–Pd and In–Pt scattering was also confirmed for In K-edge with consistent interatomic distances. Notably, the sum of their *CN*s (2.0 + 2.6 = 4.6) agreed with each *CN* of Pd–In (5.2 ± 1.0) or Pt–In (4.4 ± 0.2) with error bars. These results strongly suggest that part of Pd in PdIn was replaced with Pt to form the $(Pd_{1-x}Pt_x)In$ pseudo-binary alloy structure. Considering that there is a small contribution of Pt–Pt scattering with the interatomic distance identical to that of Pt foil, it is possible that only a

Table 1. Results of EXAFS curve-fitting for Pd–Pt–In /Al_2O_3 and reference foils.

Sample	Shell	*CN*	*R* / Å	σ^2 / Å^2	R-factor
Pd foil	Pd–Pd	12.0 (fix)	2.74 ± 0.00	0.006	0.002
Pt foil	Pt–Pt	12.0 (fix)	2.77 ± 0.00	0.005	0.000
In foil	In–In	4.0 (fix)	3.15 ± 0.01	0.017	0.008
	In–In	8.0 (fix)	3.30 ± 0.02	0.024	
Pd–Pt–In /Al_2O_3	Pd–In	5.2 ± 1.0	2.72 ± 0.01	0.013	0.018
	Pt–In	4.4 ± 0.2	2.69 ± 0.00	0.011	0.008
	Pt–Pt	2.5 ± 0.4	2.76 ± 0.01	0.010	
	In–O	1.3 ± 1.4	2.16 ± 0.02	0.010	
	In–Pt	2.6 ± 1.5	2.71 ± 0.02	0.011	0.013
	In–Pd	2.0 ± 0.4	2.72 ± 0.02	0.011	

small amount of Pt was not included in the pseudo-binary alloy but formed monometallic Pt nanoparticles. Therefore, the Pt content *x* in ($Pd_{1-x}Pt_x$)In should be slightly lower than 0.5. For the In K-edge, only a small contribution of In–O bond was detected. Because most In species are metallic, as observed in the XANES spectrum, the In–O bond can be attributed to the interaction with lattice oxygen of the Al_2O_3 support or InOx species that did not participate in the formation of ($Pd_{1-x}Pt_x$)In. Such metal–oxygen interactions with the support have previously reported.[9, 12] On the basis of the above-mentioned results, we concluded that the nanoparticulate ($Pd_{1-x}Pt_x$)In pseudo-binary alloy ($x \lesssim 0.5$) was formed on the Al_2O_3 support. We also performed temperature-programed reduction (TPR) of PdIn/Al_2O_3 and Pd–Pt–In/Al_2O_3 using H_2 and CO as reductants to compare the reducibility of In. Both TPR profiles for Pd–Pt–In showed that the reduction peaks assignable to In species shifted to much lower temperatures than those for PdIn (Figure S4), which demonstrated that the incorporation of Pt into PdIn considerably accelerates the reduction of In.

The prepared Al_2O_3-supported catalysts were tested in NO–CO–O_2 reaction at 350 °C with various O_2 concentration (0–7500 ppm; $0.75 \leq \lambda 1.5$, Figure 4a) as a model reaction. Monometallic Pd and PdIn showed high catalytic performances under rich ($\lambda = 0.75$) and stoichiometric ($\lambda = 1.0$) conditions, whereas they considerably decreased under lean conditions ($\lambda = 1.25$ and 1.5). This occurred because both NO conversion and N_2 selectivity decreased (Figure S5). The significant decrease in N_2 selectivity for PdIn is probably due to the loss of metallic In and its oxyphilic character for N_2O decomposition owing to excess O_2. However, Pd–Pt–In exhibited a remarkably higher performance under lean conditions. Considering that Pt/Al_2O_3 had very low catalytic performances over all O_2 concentrations, the enhanced activity of Pd–Pt–In cannot be attributed to the catalysis of Pt itself. However, Pd–Pt–In/Al_2O_3 showed poor catalytic activity under rich and stoichiometric conditions. The decrease in the catalytic performance under the lower λ conditions can be explained

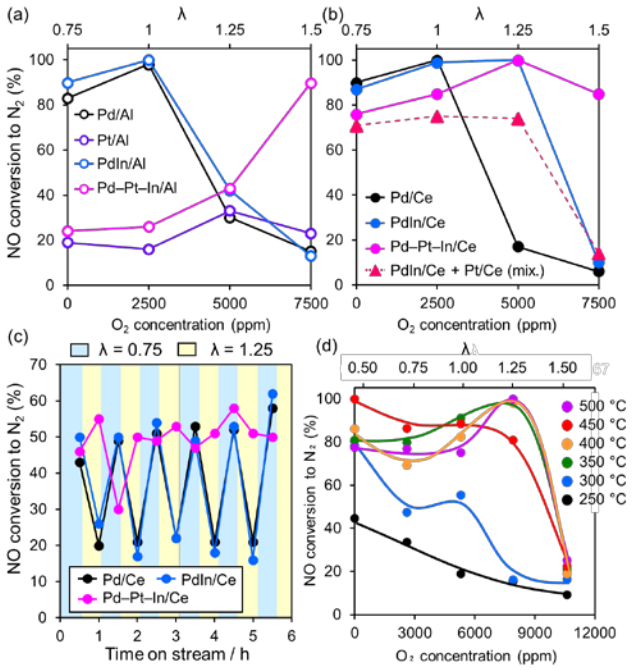

Figure 4. NO conversion to N_2 obtained in NO–CO–O_2 reaction at 350 °C with various O_2 concentrations using (a) Al_2O_3- and (b) CeO_2-supported catalysts. Reaction condition: NO = 5,000 ppm, CO = 10,000 ppm, O_2 = 0–7,500 ppm, and GHSV = 40,000 h^{-1}. Catalytic performance (c) of Pd–M/CeO_2 catalysts in NO–CO–O_2 reaction after five rich–lean cycles (1 h per each cycle) at 300 °C and (d) of Pd–Pt–In/CeO_2 catalyst in NO–CO–O_2–C_3H_6 reaction with various O_2 concentrations and reaction temperatures.

by low CO conversion (Figure S5b). Strong CO adsorption to Pt and oxygen trapping by In may be hamper the CO oxidation process under lean conditions, which lowers the overall catalytic performance. Thus, we further modified the catalysts by changing the support from Al_2O_3 to CeO_2. The oxygen releasing capability of CeO_2 can promote CO oxidation even under rich conditions.[15] The prepared CeO_2-based catalysts (Pd, Pt, PdIn, and Pd–Pt–In) had high noble metal dispersion (typically 60%–74%, Table S1). The HAADF–STEM–EDX analysis for Pd–Pt–In/CeO_2 showed that Pd, Pt, and In were homogeneously distributed on CeO_2 without aggregation (Figure S6). NO conversion to N_2 using various CeO_2-supported catalysts in NO–CO–O_2 reaction, is shown in Figure 4b. Pd/CeO_2 and PdIn/CeO_2 showed trends similar to those of Al_2O_3-supported catalysts, whereas PdIn/CeO_2 exhibited good performance at λ =1.25. This might be explained by the oxygen-storage ability of CeO_2, which could promote the reduction of InO_x to metallic In by Pd. This effect may be lost under the sever lean condition (λ =1.5), probably because CeO_2 is fully oxidized. For Pd–Pt–In/CeO_2, the catalytic performance under rich and stoichiometric conditions drastically improved, which resulted in high NO_x removal efficiencies over a wide range of oxygen concentration window of $0.75 \leq \lambda \leq 1.5$. We also performed a control experiment using a physical mixture of PdIn/CeO_2 and Pt/CeO_2, which resulted in a much lower NO conversion to N_2 under lean conditions. This result demonstrates that Pd, Pt, and In should be adjacent on an atomic scale, and that the ($Pd_{1-x}Pt_x$)In pseudo-binary alloy structure is crucial for the efficient NO_x removal under lean conditions. Then, a rich–lean cycle test was conducted to evaluate stability under

continuous operation. Figure 4c shows NO conversion to N_2 during the rich–lean cycle in NO–CO–O_2 reaction (λ = 0.75 for 0.5 h + λ =1.25 for 0.5 h) repeated six times for the Pd-based CeO_2-supported catalysts. Note that the reaction temperature was set to 300 °C so that catalytic performances were compared under near-kinetic conditions. The Pd–Pt–In/CeO_2 catalyst steadily exhibited good catalytic performance under rich and lean conditions for the first time, whereas other catalysts showed large fluctuation in conversion with a sharp decrease under lean conditions (Figure 4c). This result indicates that the high NO_x removal efficiency in a wide range of oxygen concentration window retained during the continuous deNO_x operation. The catalytic performance of Pd–Pt–In/CeO_2 was also tested in NO–CO–O_2–C_3H_6 ($0.47 \le \lambda \le 1.53$) reaction as a model reaction for TWC conditions. High NO conversions to N_2 (80%–100%) were obtained under various O_2 concentration and temperature regions ($0.47 \le \lambda \le 1.26$, 350–500 °C, Figure 4d). We also performed the TWC reaction in the presence of moisture (0.6%). Excellent catalytic performances (mostly 100% NO conversion to N_2) were obtained in a wide range of temperature (300∼500°C), GHSV (40,000–120,000 h^{-1}), gas composition ($0.47 \le \lambda \le 1.25$) (Figure S7), and in a long-term lean-rich cycle test (8 h, Figure S8), demonstrating the potential applicability of Pd–Pt–In/CeO_2 in practical use. The catalytic performances of Pd–Pt–In/CeO_2 and reported catalysts are listed in Table S3, which highlights the superiority of Pd–Pt–In/CeO_2.

In summary, we prepared trimetallic Pd–Pt–In alloy catalysts using Al_2O_3 and CeO_2 as supports and tested their catalytic performance in NO reduction with various O_2 concentrations. The resulting alloy nanoparticles have the $(Pd_{1-x}Pt_x)In$ pseudo-binary alloy ($x \lesssim 0.5$) structure, in which part of Pd in intermetallic PdIn was replaced with Pt. Pd–Pt–In/Al_2O_3 catalyzed well the NO reduction to N_2 under lean conditions and not under rich and stoichiometric conditions. Instead, the use of CeO_2 as a support considerably improves the catalytic performance under these conditions, which allows high NO_x removal efficiencies in a wide range of oxygen concentrations (NO conversion to N_2: 80%–100%, $0.75 \le \lambda \le 1.5$, 350 °C). The Pd–Pt–In/CeO_2 catalyst also retains high catalytic performance during rich–lean cycles. Pt considerably promotes the reduction of InO_x to metallic In, which allows to maintain the high NO_x removal ability of intermetallic PdIn even in the presence of excess oxygen. The results obtained in this study demonstrate a highly efficient catalytic system and a new catalyst design concept for NO_x removal under lean conditions.

ASSOCIATED CONTENT

Supporting Information. Experimental details, XRD patterns, XASF spectra, catalytic performances, and comparison with reported catalysts. This material is available free of charge via the Internet at http://pubs.acs.org.

AUTHOR INFORMATION

Corresponding Author

Shinya Furukawa − Institute for Catalysis, Hokkaido University, Sapporo 001-0021, Japan; Elements Strategy Initiative for Catalysts and Batteries, Kyoto University, Kyoto 615-8520, Japan; orcid.org/0000-0002-2621-6139; Phone: +81-11-706-9162; Email: furukawa@cat.hokudai.ac.jp

Author Contributions

The manuscript was written through contributions of all authors.

Notes

The authors declare no competing financial interest.

ACKNOWLEDGMENT

This work was supported by JSPS KAKENHI (Grant Numbers 17H01341 and 17H04965) and by MEXT project Element Strategy Initiative (JPMXP0112101003), as well as by the JST CREST project JPMJCR17J3. We thank the technical staff of the Research Institute for Electronic Science, Hokkaido University for help with HAADF-STEM observation. X-ray absorption measurements were carried out at the BL-01B1 beamline of SPring-8 at the Japan Synchrotron Radiation Research Institute (JASRI; 2019A1620).

REFERENCES

(1) Monn, C., Exposure Assessment of Air Pollutants: A Review on Spatial Heterogeneity and Indoor/Outdoor/Personal Exposure to Suspended Particulate Matter, Nitrogen Dioxide and Ozone. *Atmos. Environ.* **2001**, *35*, 1-32.

(2) Wuebbles, D. J., Nitrous Oxide: No Laughing Matter. *Science* **2009**, *326*, 56-57.

(3) Hooftman, N.; Messagie, M.; Van Mierlo, J.; Coosemans, T., A Review of the European Passenger Car Regulations–Real Driving Emissions vs Local Air Quality. *Renew. Sust. Energ. Rev.* **2018**, *86*, 1-21.

(4) (a) Zheng, T.; He, J.; Zhao, Y.; Xia, W.; He, J., Precious Metal-Support Interaction in Automotive Exhaust Catalysts. *J. Rare Earth.* **2014**, *32*, 97-107; (b) Bhattacharyya, S.; Das, R. K., Catalytic Control of Automotive NO_x: A Review. *Int. J. Energ. Res.* **1999**, *23*, 351-369.

(5) Kašpar, J.; Fornasiero, P.; Hickey, N., Automotive Catalytic Converters: Current Status and Some Perspectives. *Catal. Today* **2003**, *77*, 419-449.

(6) Yim, W.-L.; Klüner, T., Promoting O_2 Activation on Noble Metal Surfaces. *J. Catal.* **2008**, *254*, 349-354.

(7) Loffreda, D.; Simon, D.; Sautet, P., Structure Sensitivity for NO Dissociation on Palladium and Rhodium Surfaces. *J. Catal.* **2003**, *213*, 211-225.

(8) (a) Doi, Y.; Haneda, M., Catalytic Performance of Supported Ir Catalysts for NO Reduction with C_3H_6 and CO in Slight Lean Conditions. *Catal. Today* **2018**, *303*, 8-12; (b) Wu, S.; Li, X.; Fang, X.; Sun, Y.; Sun, J.; Zhou, M.; Zang, S., NO Reduction by CO over TiO_2-γ-Al_2O_3 supported In/Ag Catalyst Under Lean Burn Conditions. *Chin. J. Catal* **2016**, *37*, 2018-2024; (c) Erkfeldt, S.; Petersson, M.; Palmqvist, A., Alumina-Supported In_2O_3, Ga_2O_3 and B_2O_3 Catalysts for Lean NO_x Reduction with Dimethyl Ether. *Appl. Catal. B: Environ.* **2012**, *117-118*, 369-383; (d) Li, J.; Hao, J.; Cui, X.; Fu, L., Influence of Preparation Methods of In_2O_3/Al_2O_3 Catalyst on Selective Catalytic Reduction of NO by Propene in the Presence of Oxygen. *Catal. Lett.* **2005**, *103*, 75-82; (e) Liu, Z.; Hao, J.; Fu, L.; Zhu, T.; Li, J.; Cui, X., Activity Enhancement of Bimetallic Co-In/Al_2O_3 Catalyst for the Selective Reduction of NO by Propene. *Appl. Catal. B: Environ.* **2004**, *48*, 37-48; (f) Inomata, H.; Shimokawabe, M.; Kuwana, A.; Arai, M., Selective Reduction of NO with CO in the Presence of O_2 with Ir/WO_3 Catalysts: Influence of Preparation Variables on the Catalytic Performance. *Appl. Catal. B: Environ.* **2008**, *84*, 783-789.

(9) Jeon, J.; Kon, K.; Toyao, T.; Shimizu, K.; Furukawa, S., Design of Pd-Based Pseudo-Binary Alloy Catalysts for Highly Active and Selective NO Reduction. *Chem. Sci.* **2019**, *10*, 4148-4162.

(10) Furukawa, S.; Endo, M.; Komatsu, T., Bifunctional Catalytic System Effective for Oxidative Dehydrogenation of 1-Butene and *n*-Butane Using Pd-Based Intermetallic Compounds. *ACS Catal.* **2014**, *4*, 3533-3542.

(11) Luo, J.-Y.; Meng, M.; Yao, J.-S.; Li, X.-G.; Zha, Y.-Q.; Wang, X.; Zhang, T.-Y., One-Step Synthesis of Nanostructured Pd-Doped

Mixed Oxides MO_x-CeO_2 (M= Mn, Fe, Co, Ni, Cu) for Efficient CO and C_3H_8 Total Oxidation. *Appl. Catal. B: Environ.* **2009**, *87*, 92-103.
(12) Nakaya, Y.; Miyazaki, M.; Yamazoe, S.; Shimizu, K.; Furukawa, S., Active, Selective, and Durable Catalyst for Alkane Dehydrogenation Based on a Well-Designed Trimetallic Alloy. *ACS Catal.* **2020**, *10*, 5163-5172.
(13) Kuhn, W. K.; Szanyi, J.; Goodman, D. W., CO Adsorption on Pd (111): The Effects of Temperature and Pressure. *Surf. Sci.* **1992**, *274*, L611-L618.
(14) Olsen, C.; Masel, R., An Infrared Study of CO Adsorption on Pt (111). *Surf. Sci.* **1988**, *201*, 444-460.
(15) Li, P.; Chen, X.; Li, Y.; Schwank, J. W., A Review on Oxygen Storage Capacity of CeO_2-Based Materials: Influence Factors, Measurement Techniques, and Applications in Reactions Related to Catalytic Automotive Emissions Control. *Catal. Today* **2019**, *327*, 90-115.

Table of Contents Entry